This is a repository copy of *Suppressing resonant vibrations using nonlinear springs and dampers*.

White Rose Research Online URL for this paper:
http://eprints.whiterose.ac.uk/74614/

Monograph:
Zhang, B., Billings, S.A., Tomlinson, G.R. et al. (1 more author) (2007) Suppressing resonant vibrations using nonlinear springs and dampers. Research Report. ACSE Research Report no. 956 . Automatic Control and Systems Engineering, University of Sheffield

Suppressing Resonant Vibrations Using Nonlinear Springs and Dampers

Bin Zhang[a], Stephen A. Billings[a]， Geofrey R. Tomlinson[b], and Zi-Qiang Lang[a]

[a]Department of Automatic Control and Systems Engineering, The University of Sheffield, Mappin Street, Sheffield S1 3JD, UK
[b]Department of Mechanical Engineering, The University of Sheffield, Mappin Street, Sheffield S1 3JD, UK
E-mail: {Bin.Zhang, S.Billings, g.tomlinson, Z.Lang }@sheffield.ac.uk

Department of Automatic Control and Systems Engineering

The University of Sheffield, Sheffield, S1 3JD, UK

Research Report No. 956

June 2007

Suppressing Resonant Vibrations Using Nonlinear Springs and Dampers

Bin Zhang[a], Stephen A. Billings[a]， Geofrey R. Tomlinson[b], and Zi-Qiang Lang[a]

[a]*Department of Automatic Control and Systems Engineering, The University of Sheffield, Mappin Street, Sheffield S1 3JD, UK*
[b]*Department of Mechanical Engineering, The University of Sheffield, Mappin Street, Sheffield S1 3JD, UK*
E-mail: {Bin.Zhang, S.Billings, g.tomlinson, Z.Lang }@sheffield.ac.uk

Abstract

The energy entering the resonant region of a system can be significantly reduced by introducing designed nonlinearities into the system. The basic choice of the nonlinearity can be either a nonlinear spring element or a nonlinear damping element. A numerical algorithm to compute and compare the energy reduction produced by these two types of designed elements is proposed in this study. Analytical results are used to demonstrate the procedure. The numerical results indicate that the designed nonlinear damping element produces low levels of energy at the higher order harmonics and no bifurcations in the system output response. In contrast the nonlinear spring based designs induce significant energy at the harmonics and can produce bifurcation behaviour. The conclusions provide an important basis for the design of nonlinear materials and nonlinear engineering systems.

Keywords: energy transfer; damping; harmonic balance method; vibration transmissibility; numerical analysis; dynamical systems

1. Introduction

Suppressing resonant vibration is very important to ensure appropriate running conditions and desired behaviour in many engineering systems. The standard approach for suppressing resonant vibrations is to either introduce damping or a vibration absorber which can be passive, active or a combination of both.

Recently, based on a new filtering concept known as energy transfer filtering (Billings and Lang 2002), an entirely different approach to avoiding resonant vibration was proposed (Tomlinson et al. 2006). The concept is to transfer or distribute the incoming energy in such a way that the energy entering the resonant region of the system of interest is reduced to an appropriate level by introducing a nonlinearity between the input and the system. The basic choice of the nonlinearity can be either a nonlinear spring element or a nonlinear damping element. What has not been examined in previous studies is which nonlinear element is the best choice to suppress resonant vibrations.

In this paper, a case study is investigated based on a nonlinear damping element and a nonlinear spring element. A numerical algorithm is proposed to analyse the reduction of energy at the resonance and in the overall of the system output response produced by these two types of nonlinear elements. The numerical results, which are verified by analytical methods, indicate that the nonlinear damping element produces much lower levels of energy at the higher order harmonics

and no bifurcation effects in the system output response compared with designs based on the nonlinear spring elements. The results provide an important basis for the design of nonlinear materials and nonlinear engineering systems.

2. System description

The effects of introducing a nonlinear damping element or a nonlinear spring element at the interface between the input and the output of a single degree of freedom (SDOF) system will be studied.

Consider the SDOF system shown in Figure 1. This represents a mass supported on a nonlinear spring $f_k(\cdot)$ in parallel with a nonlinear damper $f_c(\cdot)$. The mass is subjected to a harmonic excitation force of amplitude F_d, and frequency Ω, and the output of interest is the force $F_s(t)$ transmitted to the support via the nonlinear damping element or the nonlinear spring element.
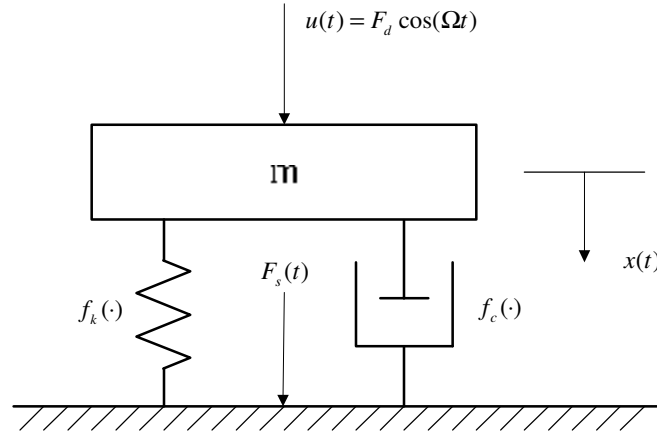

Figure 1. The SDOF mass-spring-damper system considered in the study

The equilibrium equation for the system in Figure 1 and corresponding force at the support can be expressed as

$$m\ddot{x}(t) + f_k\left[x(t)\right] + f_c\left[\dot{x}(t)\right] = F_d \cos(\Omega t) \tag{1}$$

$$F_s(t) = f_k\left[x(t)\right] + f_c\left[\dot{x}(t)\right] \tag{2}$$

For convenience, denote

$$y_d(t) = x(t) \tag{3}$$

$$y_F(t) = F_s(t) \tag{4}$$

and

$$u(t) = F_d \cos(\Omega t) \tag{5}$$

The system can then be described by a single input two output system

$$m\ddot{y}_d(t) + f_k\left[y_d(t)\right] + f_c\left[\dot{y}_d(t)\right] = u(t) \tag{6}$$

$$y_F(t) = f_k\left[y_d(t)\right] + f_c\left[\dot{y}_d(t)\right] \tag{7}$$

It will be assumed that the nonlinear damping element can be described by a linear stiffness and a

3

polynomial damping nonlinear system such that

$$f_k(\cdot) = k_1(\cdot) \tag{8}$$

$$f_c(\cdot) = c_1(\cdot) + c_3(\cdot)^3 \tag{9}$$

where k_1 is the parameter of the stiffness characteristic, while c_1, c_3 are the parameters of the damping characteristic and c_3 represents the system nonlinearity.

Substituting Eqs. (8) and (9) into Eqs. (6) and (7) yields the model of the nonlinear damping system

$$m\ddot{y}_d(t) + k_1 y_d(t) + c_1\dot{y}_d(t) + c_3\dot{y}_d^3(t) = u(t) \tag{10}$$

$$y_F(t) = k_1 y_d(t) + c_1\dot{y}_d(t) + c_3\dot{y}_d^3(t) \tag{11}$$

Similarly, it will be assumed that the nonlinear spring can be described by a polynomial stiffness and a linear damping nonlinear system such that

$$f_k(\cdot) = k_1(\cdot) + k_3(\cdot)^3 \tag{12}$$

$$f_c(\cdot) = c_1(\cdot) \tag{13}$$

where c_1 is the parameter of the damping characteristic, and k_1, k_3 are the parameters of the stiffness characteristic, and k_3 represents the system nonlinearity.

Substituting Eqs. (12) and (13) into Eqs. (6) and (7) gives the model of the nonlinear spring system

$$m\ddot{y}_d(t) + k_1 y_d(t) + k_3 y_d^3(t) + c_1\dot{y}_d(t) = u(t) \tag{14}$$

$$y_F(t) = k_1 y_d(t) + k_3 y_d^3(t) + c_1\dot{y}_d(t) \tag{15}$$

3. Analytical methods

In the analysis of a nonlinear spring with cubic stiffness described by Eqs. (5) and (14), many authors (Stoker 1950, Tamura et al. 1981, 1986, Liu et al. 2006) have used the method of harmonic balance. This approach assumes that the response may be written as a truncated Fourier series and a series solution is obtained as follows

$$y_d(t) = \overline{Y}_{d0} + \sum_{i=1}^{N_d}\left[\overline{Y}_{d(2i-1)}\cos(i\Omega_n t) + \overline{Y}_{d(2i)}\sin(i\Omega_n t)\right]$$

$$= Y_{d0} + \sum_{i=1}^{N_d} Y_{di}\cos(i\Omega_n t + \varphi_i) \tag{16}$$

where Ω_n is the natural frequency of the response and N is the number of overall harmonics used in the truncated Fourier series expansion.

Urabe and Reiter (1965, 1966) have discussed properties such as existence and convergence of the series solution. Should the response have the same period as the excitation force, then the series contains only odd harmonics of the excitation frequency and there is no constant term Y_{d0}. In this case, setting $N_d = 1$, substituting Eq. (16) into Eq. (14) and equating coefficients of the cosines and sines at the natural frequency leads to the following algebraic equations for the two-term series:

$$\left(m\Omega^2 Y_{d1} - k_1 Y_{d1} - \frac{3}{4}k_3 Y_{d1}^3\right)\sin\varphi_1 - c_1\Omega Y_{d1}\cos\varphi_1 = 0 \tag{17}$$

$$-\left(m\Omega^2 Y_{d1} - k_1 Y_{d1} - \frac{3}{4}k_3 Y_{d1}^{3}\right)\cos\varphi_1 - c_1\Omega Y_{d1}\sin\varphi_1 = F_d \tag{18}$$

Squaring and adding Eqs. (17) and (18) yields

$$Y_{d1}^{2}\left[\left(-m\Omega^2 + k_1 + \frac{3}{4}k_3 Y_{d1}^{2}\right)^{2} + c_1^{2}\Omega^2\right] = F_d^{2} \tag{19}$$

That is

$$\frac{9}{16}k_3^{2}Y_{d1}^{6} + \frac{3}{2}k_3\left(k_1 - m\Omega^2\right)Y_{d1}^{4} + \left[\left(c_1\Omega\right)^2 + \left(k_1 - m\Omega^2\right)^{2}\right]Y_{d1}^{2} - F_d^{2} = 0 \tag{20}$$

For a given amplitude of excitation F_d, this is a third degree polynomial in Y_{d1}^{2}. Real valued amplitudes of Y_{d1} are the only solutions which are physically meaningful. Depending on the value of Ω, this equation can have either one or three real roots, among which only two are stable and realizable. This leads to jump phenomena in the response as Ω passes through the bifurcation points and the amplitude switches between these two stable branches of solutions (Friswell and Penny 1994, Worden and Tomlinson 2001). The bifurcation points can be obtained by solving the equation

$$\Delta = 4a_2^{3}a_4 - a_2^{2}a_3^{2} + 4a_1 a_3^{3} - 18a_1 a_2 a_3 a_4 + 27a_1^{2}a_4^{2} = 0 \tag{21}$$

where

$$a_3 = \frac{9}{16}k_3^{2}$$

$$a_2 = \frac{3}{2}k_3\left(k_1 - m\Omega^2\right) \tag{22}$$

$$a_1 = \left(c_1\Omega\right)^2 + \left(k_1 - m\Omega^2\right)^{2}$$

$$a_0 = -F_d^{2}$$

Similarly, the transmitted force $y_F(t)$ can also be written as

$$y_F(t) = Y_{F0} + \sum_{i=1}^{N_F} Y_{Fi}\cos\left(i\Omega_n t + \theta_i\right) \tag{23}$$

If the response has the same period as the excitation force then

$$Y_{F0} = 0 \tag{24}$$

In this case, setting $N_F = 1$ and $N_d = 1$, substituting Eqs. (16) and (23) into Eq. (15) and equating coefficients of the cosines and sines at the natural frequency leads to the following algebraic equations for the two-term series:

$$\left(k_1 Y_{d1} + \frac{3}{4}k_3 Y_{d1}^{3}\right)\cos\varphi_1 - c_1\Omega Y_{d1}\sin\varphi_1 = Y_{F1}\cos\theta_1 \tag{25}$$

$$-\left(k_1 Y_{d1} + \frac{3}{4}k_3 Y_{d1}^{3}\right)\sin\varphi_1 - c_1\Omega Y_{d1}\cos\varphi_1 = -Y_{F1}\sin\theta_1 \tag{26}$$

Squaring and adding Eqs. (25) and (26) yields

$$Y_{F1} = Y_{d1} \left[\left(k_1 + \frac{3}{4} k_3 Y_{d1}^2 \right)^2 + c_1^2 \Omega^2 \right]^{\frac{1}{2}} \tag{27}$$

Solving Eq. (20) and then substituting Y_{d1} into Eq. (27) yields the magnitude of the transmitted force. Eq. (27) indicates that Y_{F1} is a single-valued function of Y_{d1}. That is, to each value of Y_{d1} there is a unique value of Y_{F1}. Therefore, bifurcations also occur in the response of transmitted force $y_F(t)$, and the bifurcation points in the response of $y_F(t)$ are the same as those in the response of $y_d(t)$.

It should be pointed out that the dynamical jumps occur at different locations when increasing and decreasing the frequency of the excitation force, but this study is focused on the situation when the frequency is decreasing. The analysis for the case when the frequency is increasing can be performed in a similar manner.

Following the analysis for the nonlinear spring, the amplitude-frequency relationship of the nonlinear damper described by Eqs. (5), (10) and (11) can be obtained as

$$Y_{d1}^2 \left[\left(k_1 - m\Omega^2 \right)^2 + \left(c_1 \Omega + \frac{3}{4} c_3 \Omega^3 Y_{d1}^2 \right)^2 \right] = F_d^2 \tag{28}$$

$$Y_{F1} = Y_{d1} \left[k_1^2 + \left(c_1 \Omega + \frac{3}{4} c_3 \Omega^3 Y_{d1}^2 \right)^2 \right]^{\frac{1}{2}} \tag{29}$$

Eq. (28) can also be written as

$$\frac{9}{16} c_3^2 \Omega^6 Y_{d1}^6 + \frac{3}{2} c_1 c_3 \Omega^4 Y_{d1}^4 + \left[\left(c_1 \Omega \right)^2 + \left(k_1 - m\Omega^2 \right)^2 \right] Y_{d1}^2 - F_d^2 = 0 \tag{30}$$

Solving Eqs. (20), (27) and Eqs. (30), (29) gives the magnitude of the response for the nonlinear spring and the nonlinear damper respectively. But since these results are based on the two-term series, which includes just the terms at the excitation frequency in the Fourier series, the value calculated is only an estimation of the real magnitude. The computation of this is discussed in section 4.

4. Numerical methods

The real magnitude of the system response can be obtained using numerical methods. At first, solving Eqs. (10), (11) or Eqs. (14), (15) gives the nonlinear damping/spring element time domain output $y_F(t)$ at a given excitation. Then performing a FFT operation on the system output and the peak magnitude of the spectrum, denoted by $\max \{ 2|Y_F(j\Omega)| \}$, yields the value predicting by the harmonic balance method.

Notice that $2|Y_F(j\Omega)|$ not $|Y_F(j\Omega)|$ is used because $2|Y_F(j\Omega)|$ represents the physical magnitude of the system output $y_F(t)$ at the frequency Ω.

In order to contrast the reduction effects of the nonlinear damping element and nonlinear spring element, an algorithm to obtain the nonlinearity and jump frequency of the nonlinear spring element under a given maximum peak magnitude is proposed as follows:

(i) Set $i=1$, $k_3=0$, $\Omega_i^{jump}=\Omega_n$, and obtain the maximum peak magnitude (denoted by Y_{FM}) for the nonlinear damper element of a given nonlinearity (that is $c_3=c$, where c is a given constant) at a number of excitation frequencies using the numerical method;

(ii) Increase the nonlinearity k_3 and compute the peak magnitude $\max\left\{2\left|Y_F\left(j\Omega_i^{jump}\right)\right|\right\}$ until $\max\left\{2\left|Y_F\left(j\Omega_i^{jump}\right)\right|\right\}=Y_{FM}$ when $k_3=\bar{k}_3$;

(iii) Find the jump frequency $\bar{\Omega}_{i+1}^{jump}$ by computing the spectrum $\max\left\{2\left|Y_F\left(j\Omega\right)\right|\right\}$ at a number of excitation frequencies when $k_3=\bar{k}_3$;

(iv) If $\left|\dfrac{\bar{\Omega}_{i+1}^{jump}-\bar{\Omega}_i^{jump}}{\bar{\Omega}_i^{jump}}\right|\geq\varepsilon$ then $i=i+1$, $\Omega_i^{jump}=\bar{\Omega}_i^{jump}$ and go to (ii);

(v) Output $k_3=\bar{k}_3$ and the jump frequency $\Omega^{jump}=\bar{\Omega}_{i+1}^{jump}$.
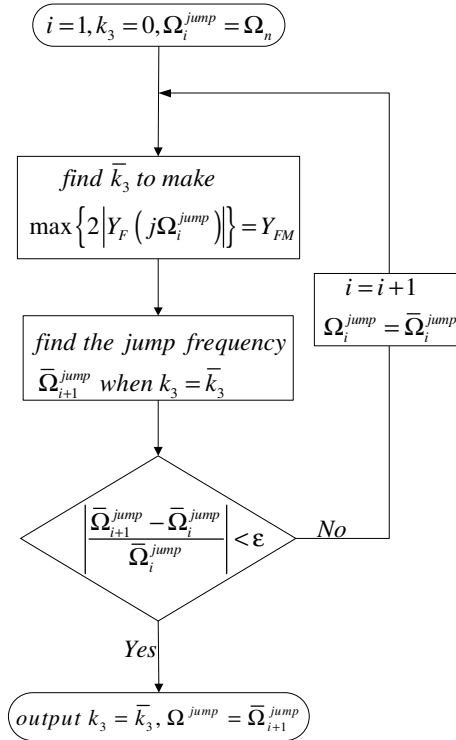
The flow diagram of this algorithm is shown in Figure 2.

Figure 2. The flow diagram of the algorithm in Section 4

5. Simulation studies

Consider the nonlinear damping element (10), (11) and nonlinear spring element (14), (15) subject to the harmonic input (5). Take the system linear characteristic and input parameters as follows:

$$m=240\text{kg}, \qquad k_1=16000\text{N/m}, \qquad c_1=29.6\text{sN/m}, \qquad F_d=100\text{N}$$

The natural frequency of the system can be given as

$$\Omega_n = \sqrt{\frac{k_1}{m}} = 8.165 \text{ rad/s}.$$

Figure 3 shows the computed peak magnitude of $y_F(t)$ of the nonlinear damping element for the case of $c_3 = 1 \times 10^3$ sN/m using the numerical and analytical methods respectively. It can be seen that the results for the two different methods match very well, which indicates that the two–term series harmonic methods work very well in this case and also confirms that the numerical method is correct.
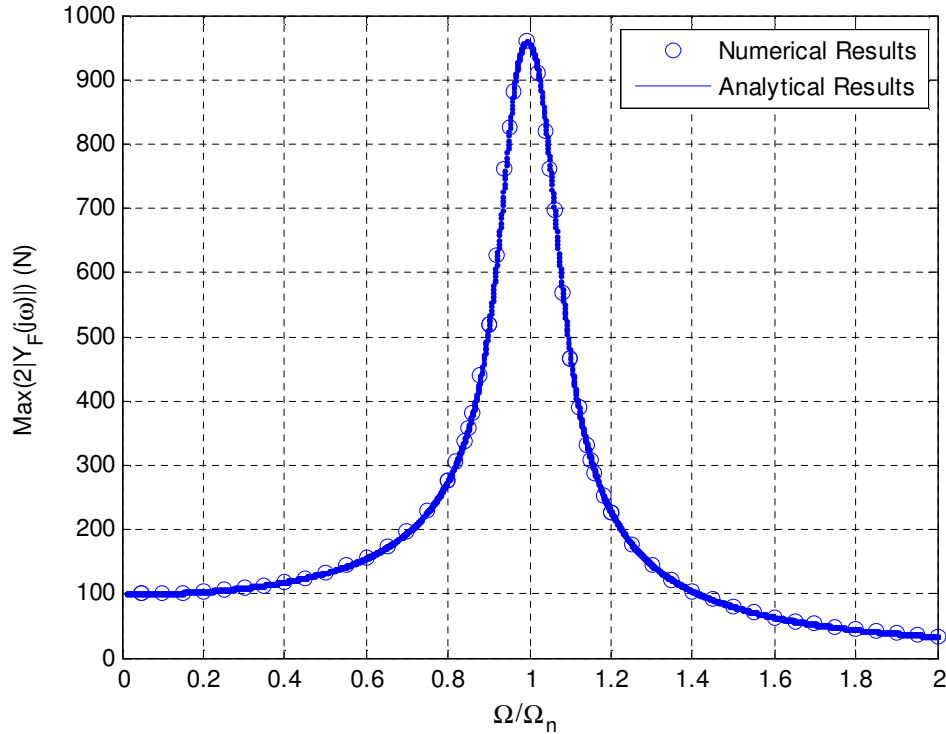

Figure 3. The peak magnitude of $y_F(t)$ for the nonlinear damping element when $c_3 = 1 \times 10^3$ sN/m. Solid lines: analytical results; circles: numerical results.

The maximum peak magnitude of $y_F(t)$ can be obtained as 959.0752N from Figure 3. Set $Y_{FM} = 959.0752$ N and then using the algorithm proposed in section 4 gives $k_3 = 2.3970945 \times 10^7$ N/m and jump frequency $\Omega^{jump} = 1.34471\Omega_n = 10.9796$ rad/s. Figure 4 shows the computed peak magnitude of $y_F(t)$ of the nonlinear spring element for the case of $k_3 = 2.3970945 \times 10^7$ N/m using the numerical and analytical methods respectively. The numerical and analytical results are in close agreement, which demonstrates that the numerical algorithm is correct. The jump frequency computed by the analytical methods is slightly different from that obtained by the numerical methods because the analytical methods are based on the two-term series. Increasing the number of terms would make the difference smaller.
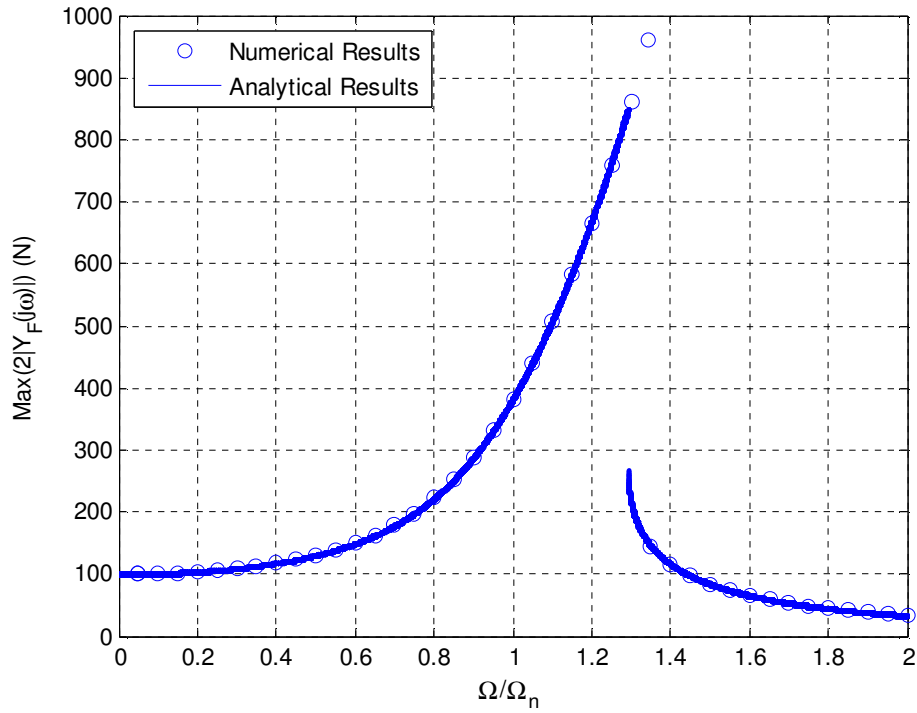
Figure 4. The peak magnitude of $y_F(t)$ for the nonlinear spring element when $k_3 = 2.3970945 \times 10^7$ N/m. Solid lines: analytical results; circles: numerical results.
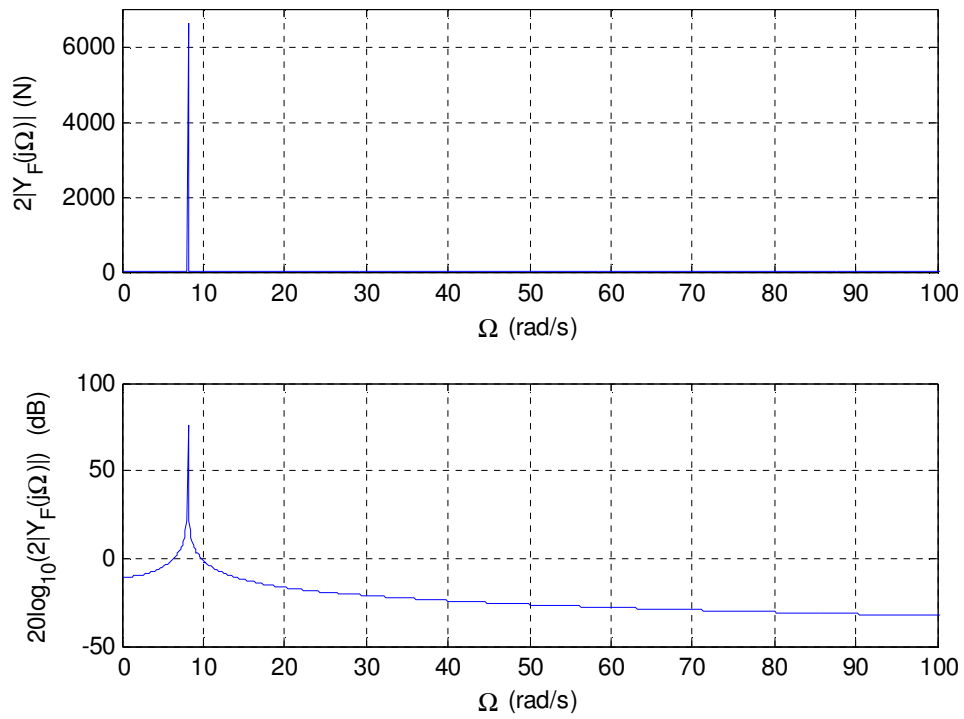

Figure 5. The spectrum and Bode response of output $y_F(t)$ for the linear system when $\Omega = \Omega_n$.
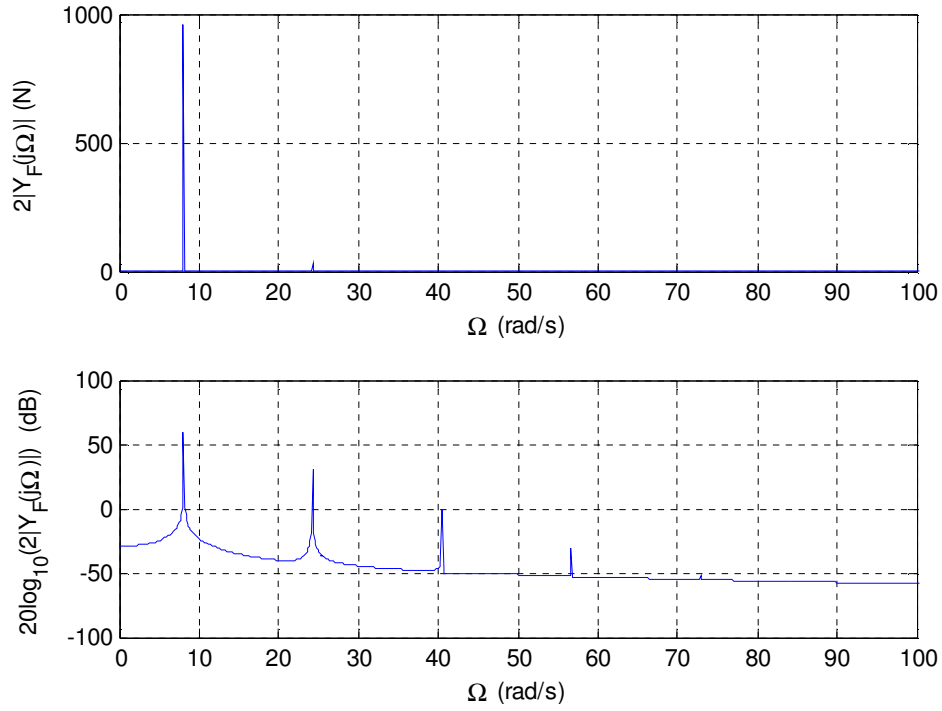
Figure 6. The spectrum and Bode response of output $y_F(t)$ for the nonlinear damping element when $\Omega = 0.99204\Omega_n$ and $c_3 = 1 \times 10^3$ sN/m.
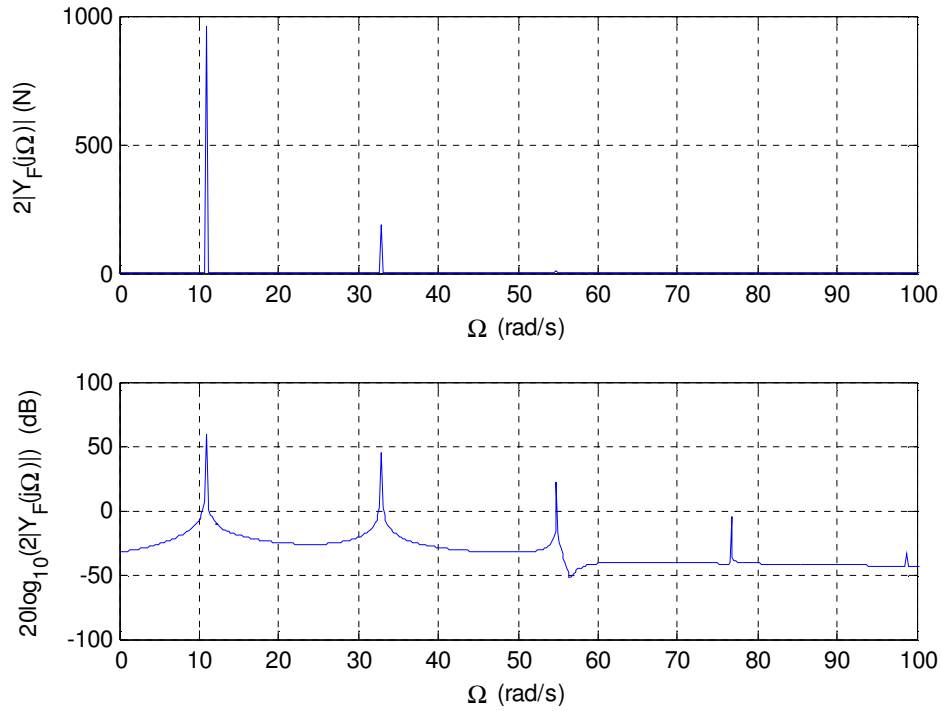

Figure 7. The spectrum and Bode response of output $y_F(t)$ for the nonlinear spring when $\Omega = \Omega^{jump}$ and $k_3 = 2.3970945 \times 10^7$ N/m.

Figure 5 shows the spectrum and Bode response of the output $y_F(t)$ for the linear system when $\Omega = \Omega_n$. The magnitude of $y_F(t)$ at the resonant frequency can be obtained as 6620.9085N from Figure 5, which indicates that the nonlinear damping element and the nonlinear spring have achieved a significant magnitude reduction percentage (MRP) given as

$$[MRP] = \frac{6620.9085 - 959.0752}{6620.9085} \times 100\% = 85.5144\% .$$

Figure 6 shows the spectrum and Bode response of the output $y_F(t)$ for the nonlinear damping element when $\Omega = \Omega_n$ and $c_3 = 1 \times 10^3$ N/m. Figure 7 shows the spectrum and Bode response of the output $y_F(t)$ for the nonlinear spring element when $\Omega = \Omega^{jump}$ and $k_3 = 2.3970945 \times 10^7$ N/m. The details of the harmonic magnitude are given in Table 1, where n is the harmonic order number and $[HMRP]_n$ (Harmonic Magnitude Relative Percentage) is defined as the percentage of the nth order harmonic magnitude relative to the dominant fundamental.

n ($n \times \Omega$)	Nonlinear Damper $f_c(\dot{x}) = c_1(\dot{x}) + c_3(\dot{x})^3$ $k_1 = 16000$ N/m, $c_1 = 29.6$ sN/m $c_3 = 1 \times 10^3$ sN/m $\Omega = 0.99204\Omega_n = 8.1$ rad/s		Nonlinear Spring $f_k(x) = k_1(x) + k_3(x)^3$ $c_1 = 29.6$ sN/m, $k_1 = 16000$ N/m $k_3 = 2.3970945 \times 10^7$ N/m $\Omega = 1.34471\Omega_n = 10.9796$ rad/s	
	Magnitude (N)	$[HMRP]_n$	Magnitude (N)	$[HMRP]_n$
1	959.0752	100.0000%	959.0752	100.0000%
2	0.0127	0.0013%	0.0579	0.0060%
3	31.7316	3.3086%	192.7520	20.0977%
4	0.0029	0.0003%	0.0306	0.0032%
5	0.9936	0.1036%	12.9116	1.3463%
6	0.0010	0.0001%	0.0110	0.0011%
7	0.0294	0.0031%	0.6071	0.0633%
8	0.0006	0.0001%	0.0088	0.0009%
9	0.0004	0.0000%	0.0196	0.0020%
10	0.0004	0.0000%	0.0070	0.0007%
11	0.0003	0.0000%	0.0072	0.0008%
12	0.0003	0.0000%	0.0058	0.0006%

Table 1. The harmonic magnitudes of output $y_F(t)$ for the nonlinear damper element under the dominant frequency excitation and the nonlinear spring element under the jump frequency excitation.

Inspection of Figure 3, 4 and 5 indicates that the nonlinear spring element can achieve the same

reduction in the output response as the nonlinear damping element but a bifurcation might occur in the nonlinear spring designed system. The bifurcation can cause a jump in the system response, which will usually not be acceptable in the engineering design. Comparing Figure 6 and 7 also shows that energy at the harmonics produced by the nonlinear spring is much higher than for the nonlinear damping element to achieve the same reduction in the resonant vibration. This can also be observed clearly from Table 1, which shows that the third order harmonic magnitude is up to 20.0977% of the dominant frequency magnitude for the nonlinear spring. This is also the reason why the two–term series harmonic method works very well in the nonlinear damping element case but not in the nonlinear spring case.

6. Conclusions

A numerical algorithm to contrast the reduction of energy in the system output response produced by designing in either a nonlinear damping element or a nonlinear spring element has been described in this study. Results from an analytical study have been used to verify the numerical method and to demonstrate the results obtained using the proposed algorithm. The numerical results indicate that the nonlinear damping element produces low levels of energy at the higher order harmonics and no bifurcations in the system output response. In contrast designs using a nonlinear spring element can produce significant energy at the harmonics and jump effects.

This study has focused on a relatively simple SDOF system to demonstrate the concepts, but the results can be extended to more general cases. The work provides an important basis for the design of nonlinear materials and nonlinear engineering systems.

Acknowledgement

References

S.A. Billings, and Z.Q. Lang, Non-linear systems in the frequency domain: energy transfer filters, International Journal of Control 75(2006) 1066-1081.

G.R. Tomlinson, Z.Q. Lang, S.A. Billings and F. Xie, Suppressing resonant vibrations via energy transfer concepts, Structural Control & Health Monitoring 13 (2006) 523-535.

J.J. Stoker, Nonlinear Vibration, New York: Interscience (1950).

H. Tamura, T. Kondou and A. Sueoka, Higher approximation of steady oscillations in nonlinear systems with single degree of freedom(suggested multi-harmonic balance method), Bulletin of the Japanese Society of Mechanical Engineers 24 (1981) 1616-1625.

H. Tamura, T. Kondou and A. Sueoka, Higher approximate solutions of the Duffing equation (odd order superharmonic resonances in the hard spring system), Bulletin of the Japanese Society of Mechanical Engineers 29 (1986) 894-901.

L. Liu, J.P. Thomas, E.H. Dowell, P. Attar and K.C. Hall, A comparison of classical and high dimensional harmonic balance approaches for a Duffing oscillator, Journal of computational physics 215 (2006) 298-320.

M. Urabe, Galerkin's procedure for nonlinear periodic systems, Archive for rational mechanics and analysis 20 (1965) 120-152.

M. Urabe, and A. Reiter, A numerical computation of nonlinear forced oscillators by Galerkin procedure, Journal of Mathematical Analysis and Applications 14 (1966) 107-140.

M. Friswell and J.E.T. Penny, The accuracy of jump frequencies in series solutions of the response of a Duffing oscillator, Journal of Sound and Vibration 169 (1994) 261-269.

K. Worden, and G.R. Tomlinson, Nonlinearity in structural dynamics: detection, identification and modelling, Bristol and Philadelphia: Institute of Physics Publishing (2001).